Addressing Complex and Axially Aligned Corrosion with MFL Technologies and the Benefits of Triaxial Methods

Anthony Tindall, Steve Farnie
Baker Hughes

Pipeline Pigging and Integrity Management Conference

February 12-16, 2024

Organized by
Clarion Technical Conferences

https://doi.org/10.52202/072781-0059

https://doi.org/10.52202/072781-0059

Abstract

It is well known that when corrosion pits interact, the interpretation of inspection data gathered by Magnetic Flux leakage tools (an indirect measurement technique) becomes challenging due to the nature of the overlapping and superimposing signal responses across the multi-defect profiles. Such "complex" corrosion is of particular concern to pipeline operators as it is these areas, particularly axially oriented, that are often the most critical to pipeline integrity. And then, being the most difficult to both interpret and size accurately, these can lead to "outliers" relative to conventional ILI specifications and industry guidelines (e.g., API 1163). Such outliers are increasingly grouped into two types, namely Safety Outliers (where defect severity is under called leading to underestimated remaining strength) or Resource Outliers (when defect severity is overcalled potentially leading to unnecessary digs).

The goal of any in-line inspection method is to represent corrosion fully and accurately on the pipe. To achieve best performance, we must be able to first detect when these complex or interacting signals occur and then, more importantly, interpret them correctly. In physics terms, the nature of MFL field leakage is a 3-dimensional vector and predictable, yet different signal responses to metal loss (and other features) are observed in each of these 3 vectors which can be quantified and characterized as an improved means to translate leakage signals to the corrosion they more accurately represent.

Single axis MFL, whether conducted with axially or circumferentially oriented magnetizers, will reach limits in its capabilities regardless of sensing resolution. MFL is a mature technology, and an operator today should expect most tools to perform to specification on isolated corrosion. However, the adoption of long proven triaxial sensors, at optimal resolution, on Magnetic Flux Leakage inspection vehicles provides an integrity engineer significant advantages to minimize potential outliers when things are not so straightforward.

This paper will outline how the three independent components of the triaxial flux leakage response provide unique identifiers for cases of axial corrosion, highly asymmetrical defects, corrosion in corrosion, wide area erosion/corrosion with pitting, to name but a few. At the same time, the additional signal components provide independent measures that enable better performance in latest generation algorithm techniques and development than those trained on fewer inputs.

The authors will present real world examples of these unique identifiers being used in practice to interpret highly complex corrosion and the latest work Baker Hughes has been conducting in close partnership with our customers with the common goal to best manage these "complex morphologies" successfully and efficiently with one inspection. "

https://doi.org/10.52202/072781-0059

Introduction

Corrosion within a pipeline occurs in varying shapes and sizes on the internal and external surfaces. For the last 25 years, the pipeline industry has relied upon the classification of defects based on their surface dimensions of length and width, as stipulated within the Pipeline Operators Forum specification in Figure 1.

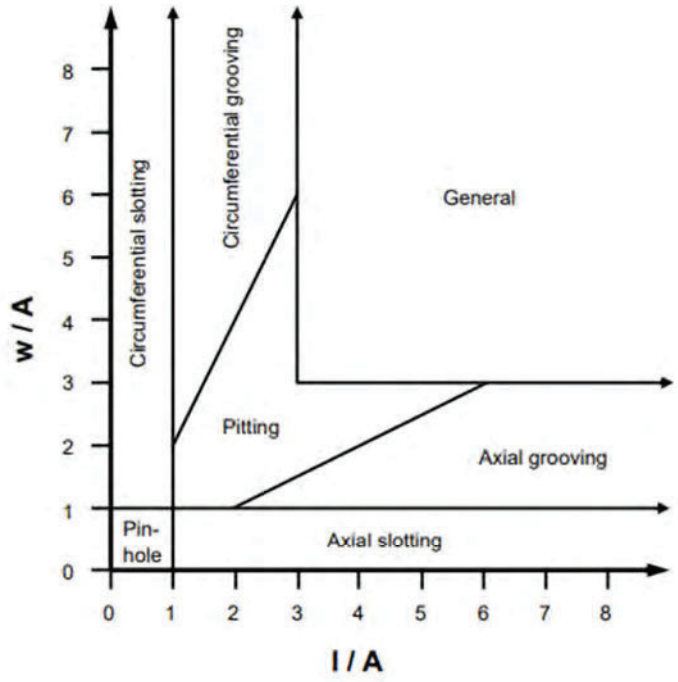

The geometrical parameter A is linked to the NDE methods in the following manner:

- If t < 10 mm then A = 10 mm
- If t ≥ 10 mm then A = t

Figure 1: POF metal loss categories [1]

This reporting standard is widely recognized and is utilised intensely within the pipeline industry around the globe.

Axial aligned corrosion would fall within the "axial slotting" and "axial grooving" categories due to the relationship between length and width. The axial features within a pipeline can vary significantly from a simplified length and width category as described by POF e.g., axial slotting = defect which is bound by having a width less then 10mm and length greater then 10mm. It is rare to find an axial feature that is isolated as a singular corrosion formation does not follow these arbitrary boundaries laid out in the POF table. Corrosion patterns vary enormously and can often appear random in their creation as seen in the laser scan example in Figure 2.

https://doi.org/10.52202/072781-0059

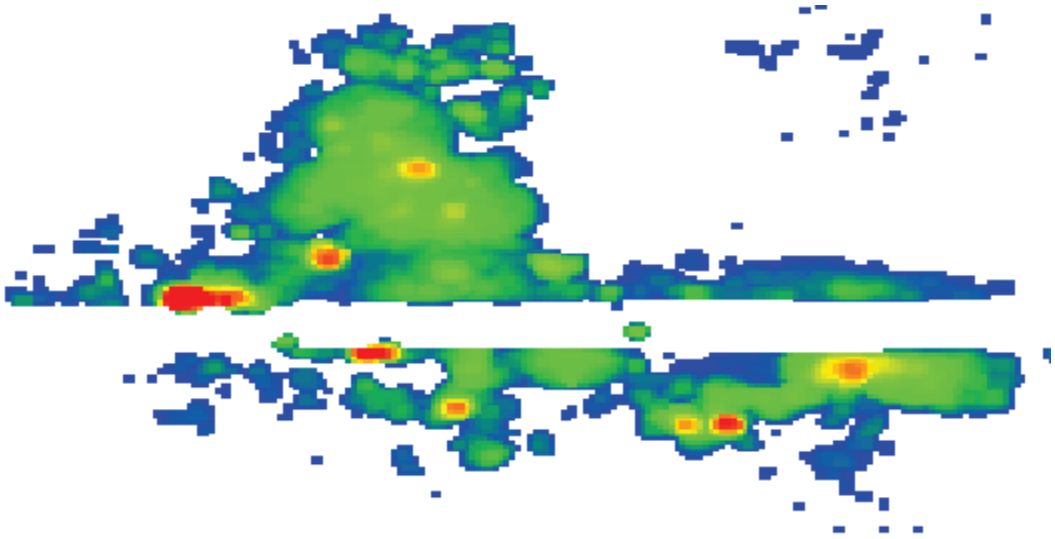

Figure 2: Laser scan containing axial slotting within complex corrosion adjacent to a seam weld

When there are additional features interacting with the axial slot, then the signal becomes more complex. This complexity increases when there are defects not only interacting with the axial slotting but also fully within its boundaries. These types of complex features are not normally specifically identified as part of an ILI inspection, since this form of complexity cannot be categorized by length and width parameters only (as per the POF categories). Therefore, operators need to be mindful that simplified specifications may have been based upon simple parabolic shapes to fit the POF specification rather than by being exposed to real corrosion that often exhibits these complex profile interactions.

Complex morphologies can pose a challenge to both axial Magnetic Flux Leakage (MFL) tools and circumferential MFL tools. Operators which have pipelines susceptible to this type of corrosion face the potential for both:

1. Safety outliers – under calling defect significance (potential of leak)
2. Resource outliers – over calling defect significance (unnecessary digs)

Baker Hughes overcomes the challenges of "complex axial slotting" by utilising the benefits that triaxial MFL data provides. Triaxial MFL data has three measurements compared to the one measurement on standard axial MFL. These three measurements are axial, radial and transverse.

By utilising triaxial MFL data and combining the different signal measurements, Baker Hughes can resolve those axial slotting defects which are complex e.g., have additional interactions. Baker Hughes' current performance example for MagneScan™ SHR+ (Super High Resolution Plus) can be seen in Figure 3 at 95% confidence level within the reporting specification.

https://doi.org/10.52202/072781-0059

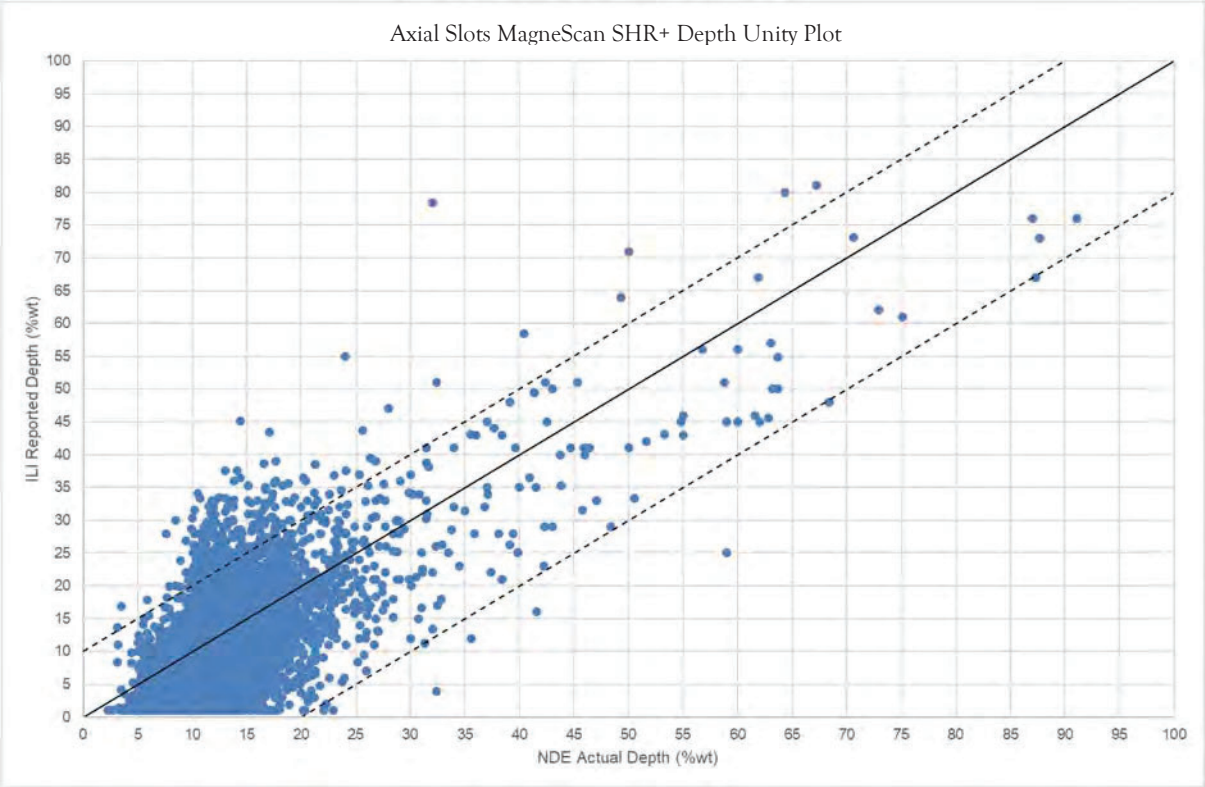

Figure 3: Baker Hughes sizing performance unity plot for axial slots

As with all methodologies there are opportunities for improvements and recent developments have focussed on those features outside of the 95% confidence area. These are considered as "outlier axial features with significant complexities". This paper focuses on the methodology and data fusion using the triaxial signal responses used to limit these "outliers", reviews the principles behind this methodology and summarises the improvements in defect predictions.

Principles of magnetic ILI and defect signals

Principles of axial MFL inspection

Axial MFL inspection, as shown in Figure 4, utilises a magnetic field introduced into the pipeline which is parallel with the pipe. All magnetic inspection vehicles are based on three basic principles:

1) A north and south magnet in contact/coupled to the pipe wall.
2) A return path on the inspection vehicle or within a sensor sledge.
3) Sensing for the detection of "Flux Leakage" from the pipe wall.

https://doi.org/10.52202/072781-0059

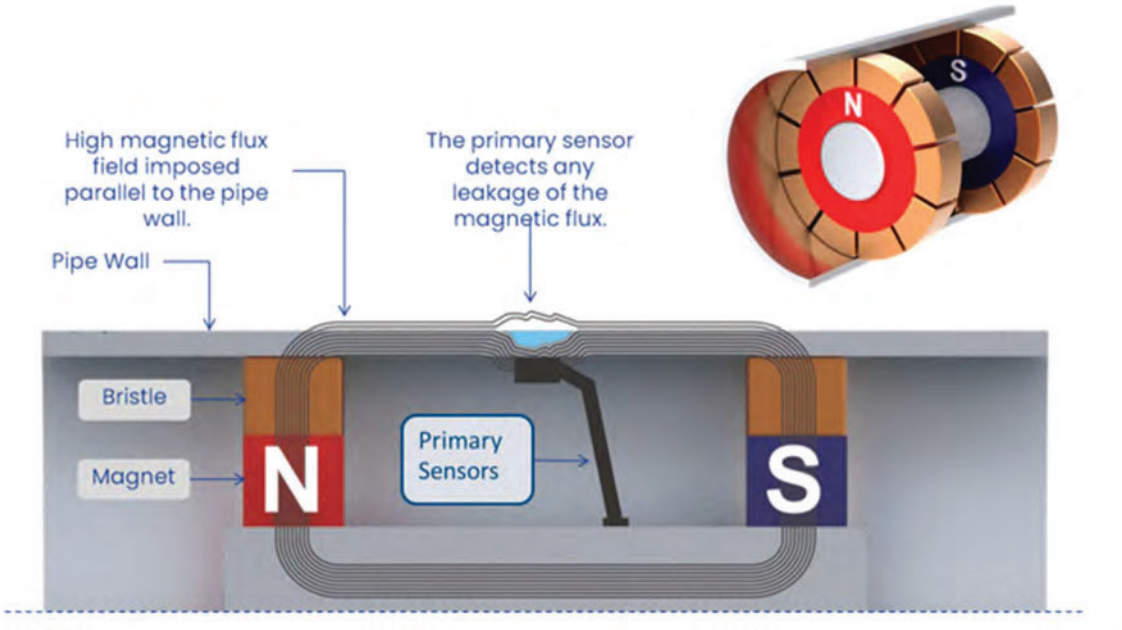

Figure 4: Axial magnetic ILI principles

How these three principles are achieved by individual ILI companies varies. Magnetic brush design allows for strong magnets and therefore increased wall thickness range and faster inspection velocities, while magnet bars are more flexible for overcoming dual diameter restrictions and are operationally more cost effective. Whichever method is adopted, then the three basic principles remain.

Principles of transverse MFL inspection

Magnetic inspection in the transverse or circumferential direction utilises the same 3 principles as the axial inspection but the magnetic field is oriented and directed around the pipe circumference, as shown in Figure 5.

https://doi.org/10.52202/072781-0059

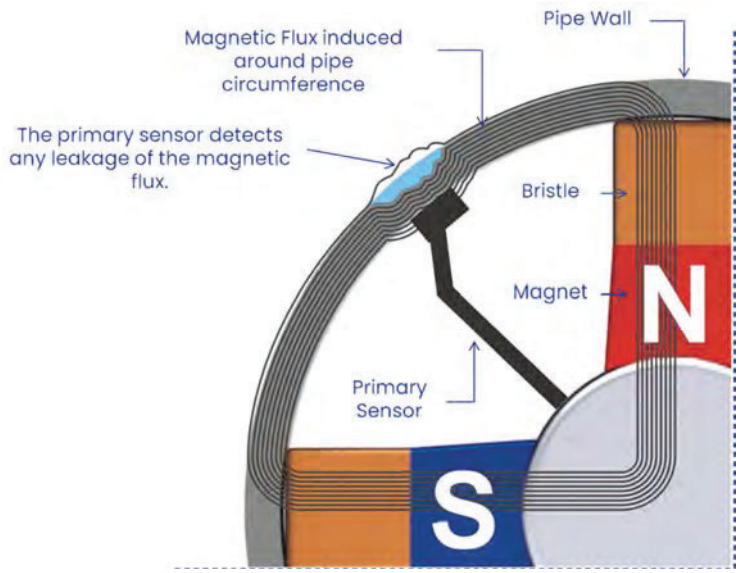

Figure 5: Transverse magnetic ILI principles

In this case, the magnetic field is aligned circumferentially around the pipe diameter. This configuration can provide additional challenges over the axial design such as variable spacings between magnets and sensors and the increased susceptibility of the imposed magnetic field strength and uniformity due to speed effects. Due to the magnetic alignment change, axial MFL and transverse MFL have different responses to non-circular corrosion defect shapes as shown in Figure 6.

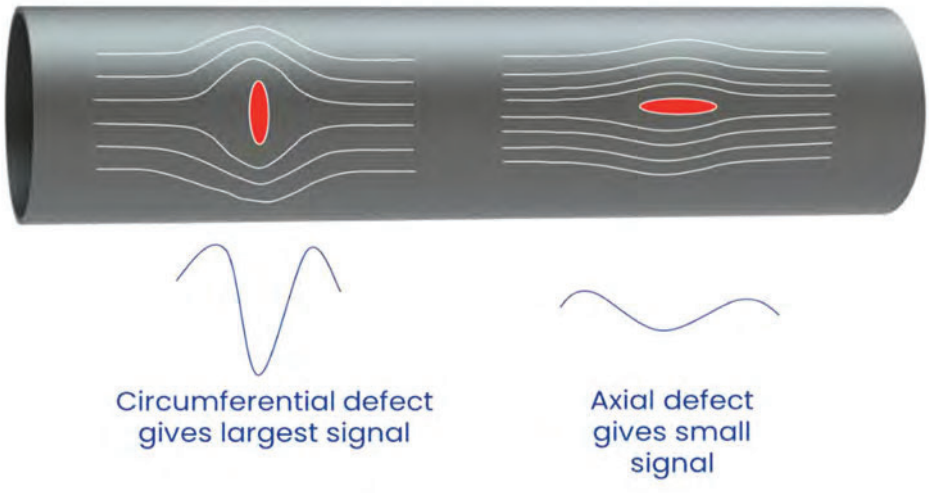

Figure 6: Axial inspection defect orientations

On axial MFL inspections the magnetic field runs parallel to the pipe. This means that any defect cutting across the field gives a high magnetic response and therefore is very sensitive to pits, general and circumferential defects as shown in Figure 7.

https://doi.org/10.52202/072781-0059

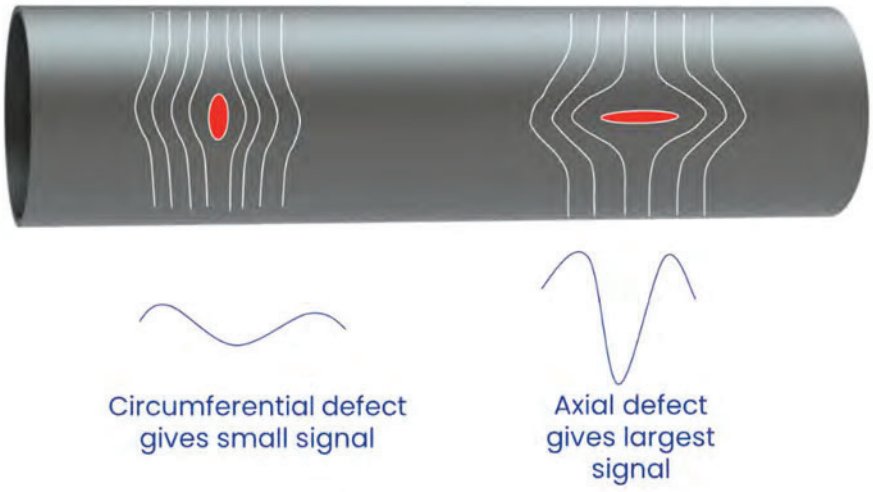

Figure 7: Transverse inspection defect orientations

On transverse MFL inspections the magnetic field runs around the circumference of the pipe. This results in any defect cutting across the field circumferentially giving a high magnetic response and therefore detection is very sensitive to axially oriented defects – primarily grooving and slotting.

A successful implementation of a sizing model will be able to compensate for the amplitude differences, so the defect shape will not necessarily result in depth outliers. However, where the defect shape is unclear, such as in interacting complex corrosion, then uncorrected amplitude changes can result in inaccurate depth predictions. Specifically, unrecognised axial areas in an axial field tool can be under called, therefore the identification and measurement of axial features within complex corrosion areas is critical. The opposite is true for transverse field tools where circumferential features will be attenuated.

Triaxial enhanced axial field measurement

Axial MFL can be enhanced significantly by utilising "Triax" sensors. Instead of only measuring the flux leakage in a single direction (typically axial), there are two additional sensors within the senor array. These measure the "radial" and "transverse" components of the magnetic field as shown in Figure 8.

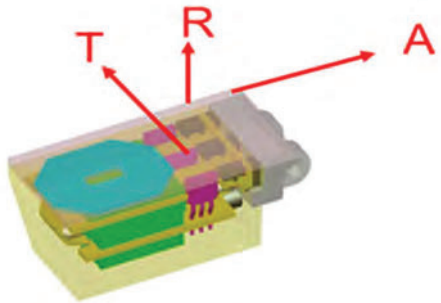

Figure 8: A triaxial sensor head showing 9 Hall effect sensors – 3 sets of triaxial sensors

https://doi.org/10.52202/072781-0059

The axial sensor measures the flux leakage i.e., volume of corrosion and its key components. For a simple pit, the signal consists of a single peak (Figure 9):

- Measured down pipe.
- Sensitive to "volumetric" losses.
- Measure nominal field strength.

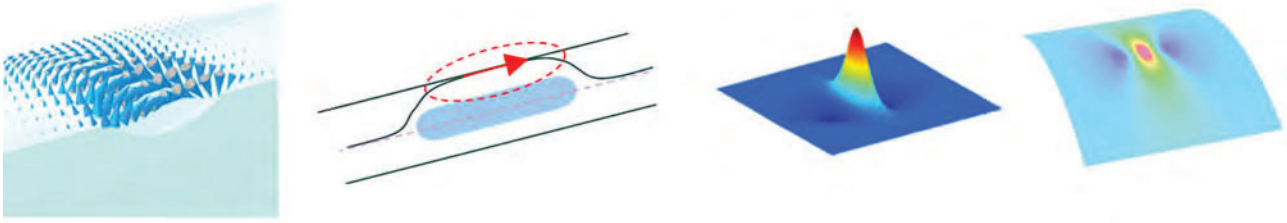

Figure 9: A typical defect signal in the axial direction

The Radial sensor measures the points and the rate of change where the field leaves the pipe and returns. For a simple defect, the signal consists of two peaks of opposite polarities (Figure 10).

- Measured out/in from centre.
- Highest sensitivity to changes in depth.
- Identifies start and end of features.

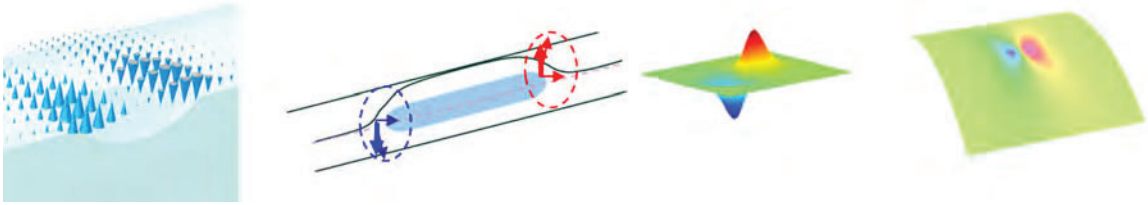

Figure 10: A typical defect signal in the radial direction

The transverse sensors measure the movement of the field around the defect. This highlights the corners or extent of a defect and the rate of change measured circumferentially around the pipe. For a simple defect, a typical signal will have four poles surrounding the peak of the defect (Figure 11).

- Added sensitivity to in-plane shape.
- Improved width measures and identification of background corrosion (larger underlying areas of corrosion) and corrosion in corrosion situations.

https://doi.org/10.52202/072781-0059

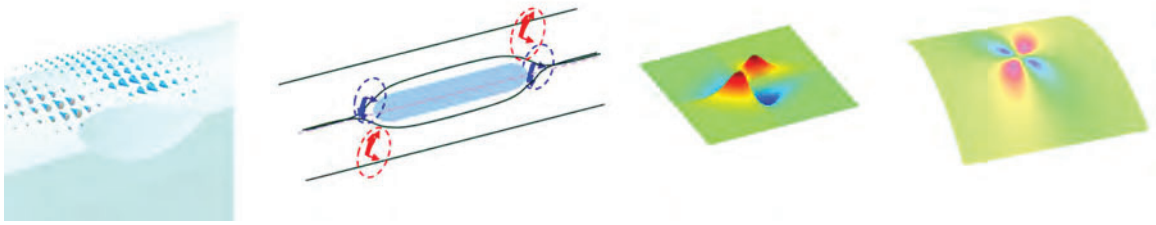

Figure 11: A typical defect signal in the transverse direction

Utilising the Triax sensors the "contextual" interactions within complex features can be more reliably identified and compensated for with specific methods within the analysis process. Whereas with axial only MFL or transverse MFL, then the signal is unable to be as reliably broken down to understand these important contextual interactions to ensure accurate depth measurement.

Overview of axially aligned corrosion identification using triaxial sensors

The theory of utilising multiple measurements from the triaxial sensors to identify complex corrosion morphology can be illustrated by considering and contrasting the signals recorded from three simple examples. In the first, Figure 12a, consider the interaction between two isolated axially aligned pits:

Figure 12a: Axially aligned pits

Figure 12b shows the magnetic response of Axial only MFL from the two pits, which can be clearly seen in trace view.

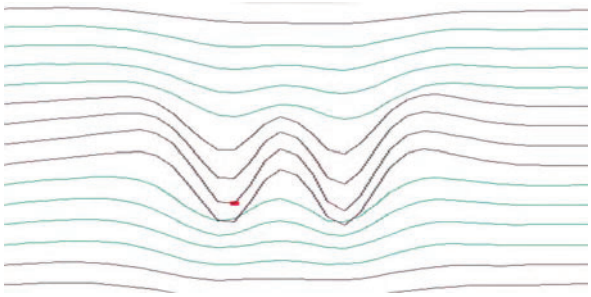

Figure 12b: Axially aligned pits – axial ILI signal

https://doi.org/10.52202/072781-0059

When analysing the radial measurement of the Triax sensor data, it is beneficial to utilise a "false colour or rainbow/heat map" view. The radial measurements are recording changes in the background field, where magnetic flux leaves the pipe and when it returns, measuring the exact location of the start and end of the flux leakage of a defect. In the false colour radial measurement from the radial sensor then start is represented by blue on the heat map, while the yellow/red represents the end of the defect.

Figure 12c shows the radial signal for the two pits. In the false colour, radial measurement from the radial sensor, start is represented by the blue on the heat map, while the yellow/red represents the end of the defect. Two pairs of "red-blue" poles can be seen, indicating that whilst the pits are close, they are not interacting.

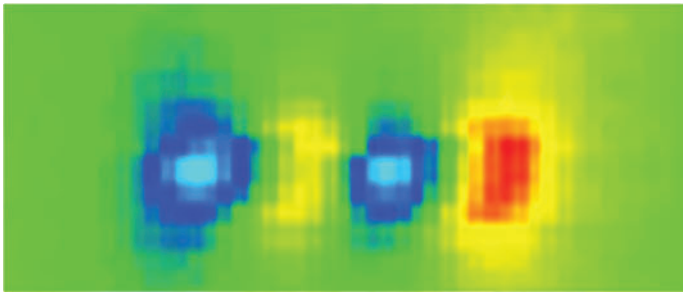

Figure 12c: Axially aligned pits – radial ILI signal

The second example is a long axial groove, machined with a constant depth (Figure 13a). Figure 13b shows the axial component signal for this feature. Note the peaks at the start and end of the signal and reduced magnetic field recorded in the centre. In some natural corrosion examples, it can be difficult to distinguish these signals from the previous example of interacting pits.

Figure 13a: Axial groove

https://doi.org/10.52202/072781-0059

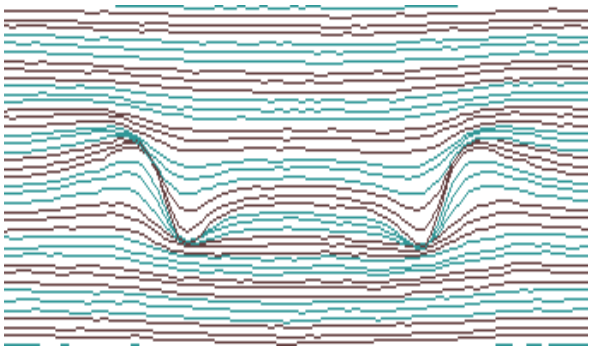

Figure 13b: Axial groove – axial ILI signal

Figure 13c shows the radial component signal for the same axial groove. The signal shows a single peak at the leading and trailing edge of the feature with the peak polarity indicating the start and end of the feature. A comparison with Figure 12c indicates how the radial component signal can unambiguously distinguish between interacting pits and continuous depth axial corrosion.

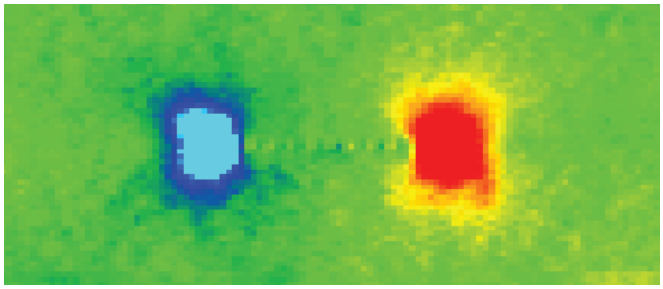

Figure 13c: Axial groove – radial ILI signal

The third example shows a slightly more complex scenario of possible defect morphology - an axial slot with an additional axial slot within it. Figure 14a shows the defect shape as-machined – sometimes referred to as a "defect-within-defect".

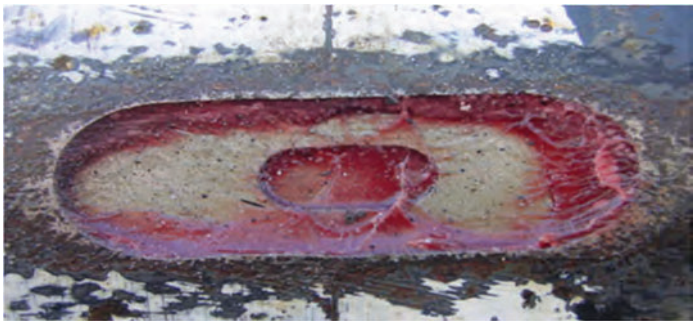

Figure 14a: Defect within defect

This is relatively a very clean defect and yet in the diagram below the axial only MFL data produces a signal based on the volume of flux leakage.

https://doi.org/10.52202/072781-0059

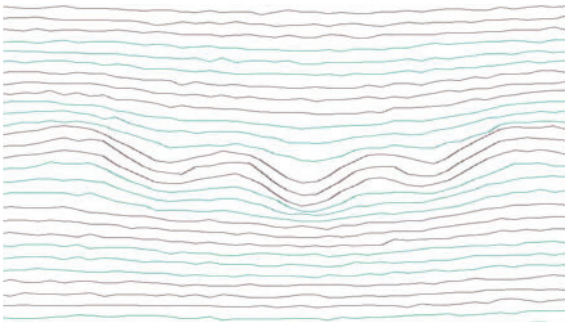

Figure 14b: Defect within defect – axial ILI signal

Figure 14b shows the axial component signal for the compound defect feature. This signal could easily be interpreted as 3 pits rather than a defect within defect. However, with the addition of the radial sensor data (Figure 14c), which measures the start and end points where there is a change in depth, then it can clearly be seen that there are in fact two defects, one inside the boundary of the other.

The radial sensor data shows a pattern of:

1. Blue (start defect)
2. Blue (start interior defect)
3. Red (end interior defect)
4. Red (end defect)

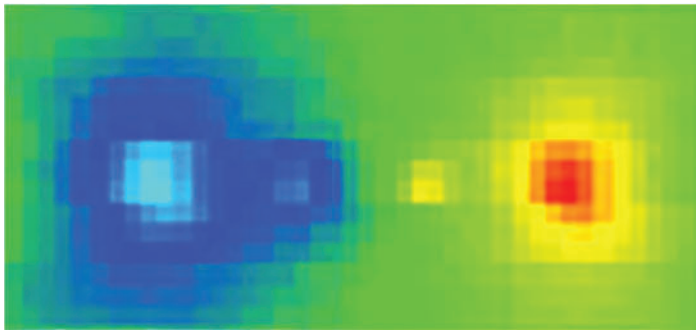

Figure 14c: Defect within defect – Radial ILI signal

This principle of identifying the start and ends of features enables huge advantages in identifying:

- Isolated axial defects
- Pinholes
- Circumferential defects
- Defects within defects (including pinholes with slots, pits in pits, etc.)

and, as will be demonstrated below, these principles can be extended to understand more complex corrosion morphologies.

https://doi.org/10.52202/072781-0059

Where inspection vehicles with axial only MFL sensors have increased the sampling resolutions both in the circumferential spacing and axial sampling over recent years, these inspection vehicles are still only a single flux leakage measurement and so the complexity within a corrosion area cannot easily be broken down and sized more accurately, namely when the risk of an outlier is greatest.

Triax sensors are deployed on all Baker Hughes VECTRA GEMINI and MagneScan axial MFL inspection tools, and having the axial, radial and transverse sensors and the accompanying analysis methodology overcomes the limitations with axial only MFL and transverse only MFL.

Outlier Performance Case Study

The following case study was carried out on a set of over 50 sites containing complex axial corrosion. All sites had associated laser scan data so accurate depths, defect morphologies and interactions could be assessed. Most of the sites had been inspected using multiple ILI technologies and were regarded as outliers – most often being under called by the axial MFL or overcalled using transverse MFL with another vendor.

The aim of the study was to see if the utilisation of the full Triax sensors and application of the Triax analysis principles described above could help to identify the axial areas and improve the depth and burst pressure performance.

Overview of complex corrosion identification using Triax sensors

Figure 15 shows a laser scan of an area of corrosion containing pits and axially aligned areas. The deepest areas, shown in yellow and red, are mostly within the axial sections.

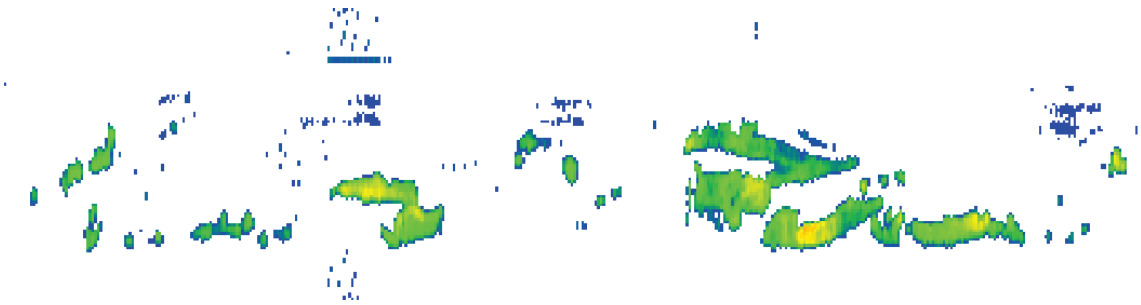

Figure 15: Axial aligned corrosion laser scan

Figure 16 illustrates the same area juxtaposed with the axial component ILI signal data of an axial MFL inspection, shown in a false colour display. An examination of the largest amplitude areas, again shown in yellow and red and highlighted on the laser scan, show they are not necessarily the deepest sections but rather where the ILI signal is amplified due to the corrosion being wide or circumferentially interacting. This is to be expected as the circumferentially aligned corrosion deflects more magnetic flux for the same metal loss volume as explained in the previous sections. In contrast, the axially orientated areas do not stand out.

https://doi.org/10.52202/072781-0059

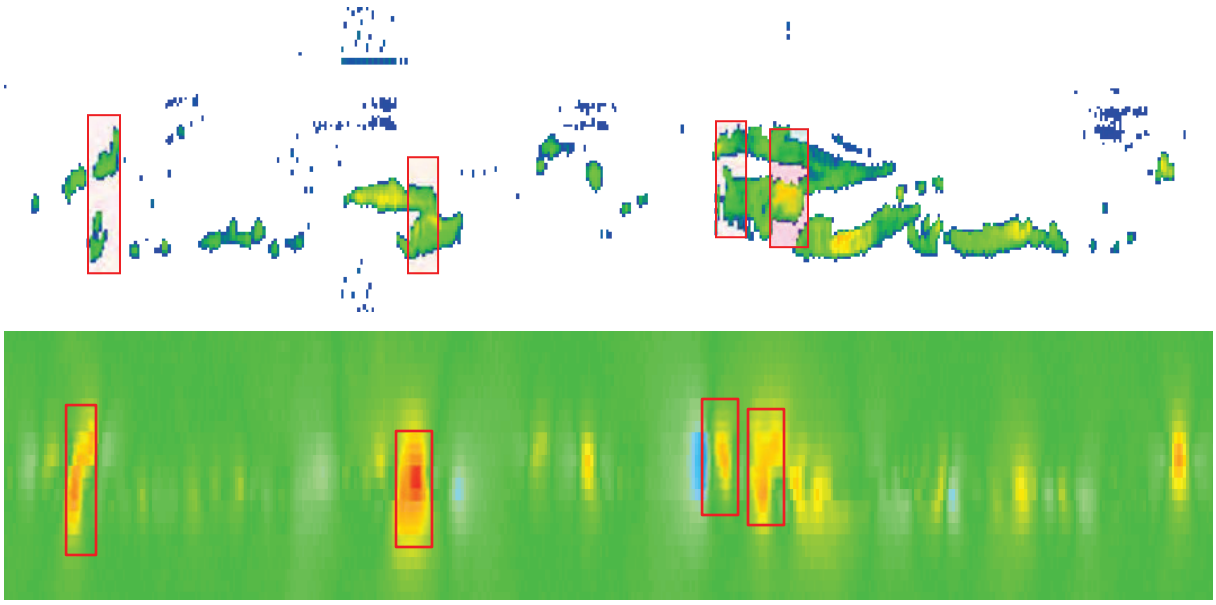

Figure 16: Axial aligned corrosion laser scan and axial component ILI signal

Utilising axial only, the axial MFL data does not help in identifying the most important aspects of the corrosion, although the trained analyst eye can already detect hints of the true nature of the features.

Figure 17 shows the same area, now with the transverse sensor ILI data. Rather than false colour, the ILI data is displayed in an "overlay" view where the simpler axial component signal is displayed in trace plot and with the transverse signal displayed in false colour.

The transverse quadripolar signal highlights the overall extents of the connected areas of corrosion. The second area is more complex as it consists of two areas with a common start point, but this is still evident as the signals in the trailing area clearly indicate only the end of a corrosion site. These can be contrasted with the self-contained signal of the isolated pit on the far right of the scan.

The quadripolar signals in the transverse visualisation indicate the areas of corrosion which can be considered connected or axial, and then assessed in more depth using the radial signal.

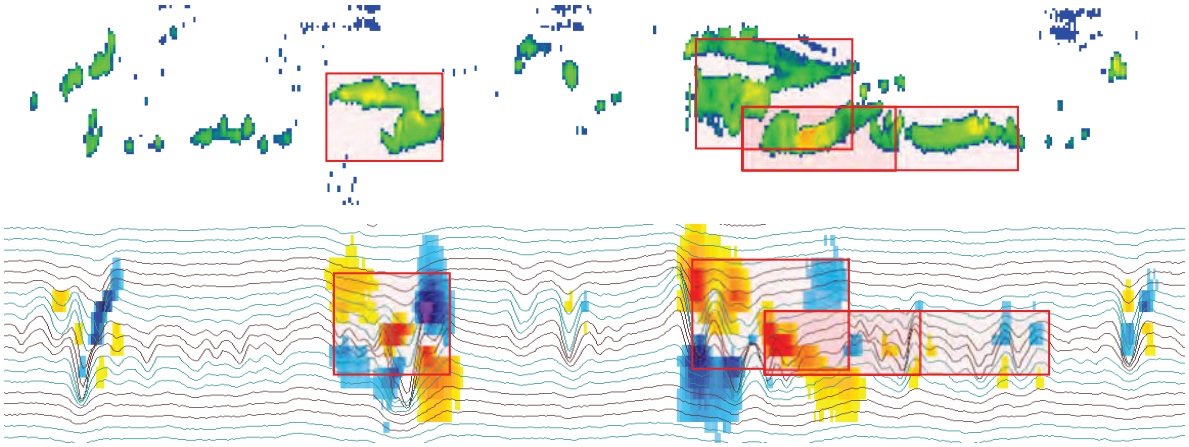

Figure 17: Axial aligned corrosion laser scan and axial component / transverse component overlay ILI signal

https://doi.org/10.52202/072781-0059

Figure 18 shows the same area, now with the radial sensor ILI data overlay. This allows the depth changes within axial areas to be visualised and quantified in more detail. The radial poles indicate magnetic flux leakage in the direction out and into the pipe wall, which can indicate respective increases and decreases in corrosion depth. The major start and end of the axial corrosion sites have been added to the diagram for clarity. In the Baker Hughes analysis software, the visualisation is adaptive to also display the finer details in the depth variations not visible below, and each aspect of the signal can be measured and utilised in the sizing process to quantify the depth variations in the corrosion.

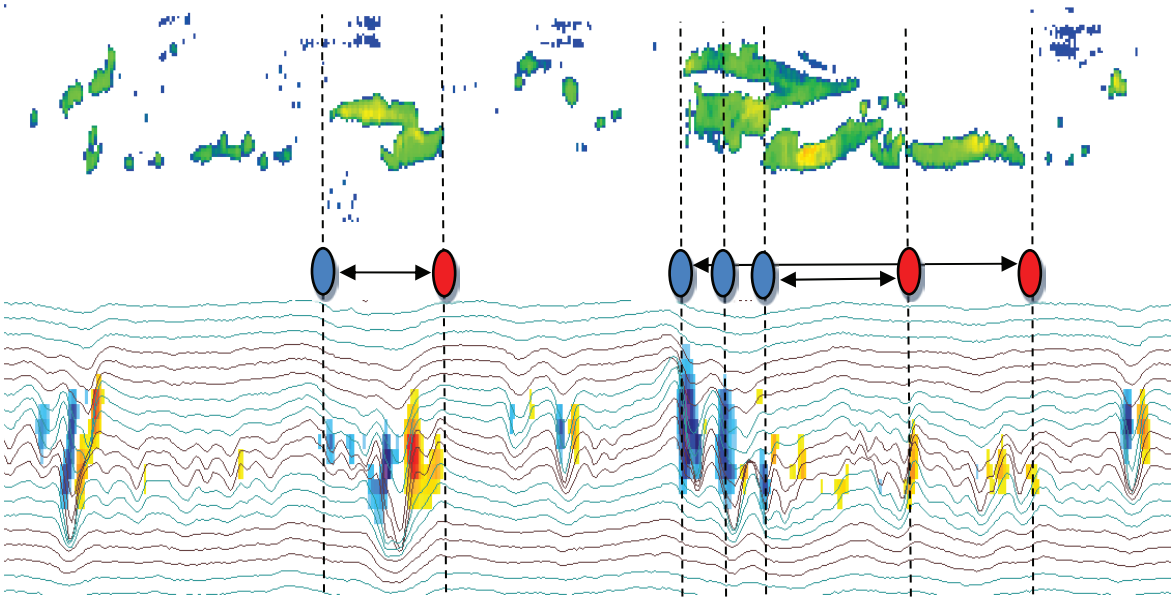

Figure 18: Axial aligned corrosion laser scan and axial component / radial component overlay ILI signal. The red/blue ellipses indicate the predominant start/end of axial corrosion areas.

Corrosion types and depth prediction

The principles described above can be applied to more complex areas. Each of the case study sections were analysed and Baker Hughes was able to categorise these into a number of more standard scenarios – or larger areas could be decomposed into a smaller section which could be categorised – and then appropriate analysis techniques could be applied to each section.

Some examples of the distinctions that must be identified for accurate categorisation and assessment are shown in the figures below. Figure 19 shows an area of corrosion which is certainly axial, but also has portions which are angled and circumferential in nature. It also shows areas of connected corrosion and dense pitting, which must be distinguished (using the principles shown in Figures 12c vs 13c) correctly for depth and pressure assessment.

https://doi.org/10.52202/072781-0059

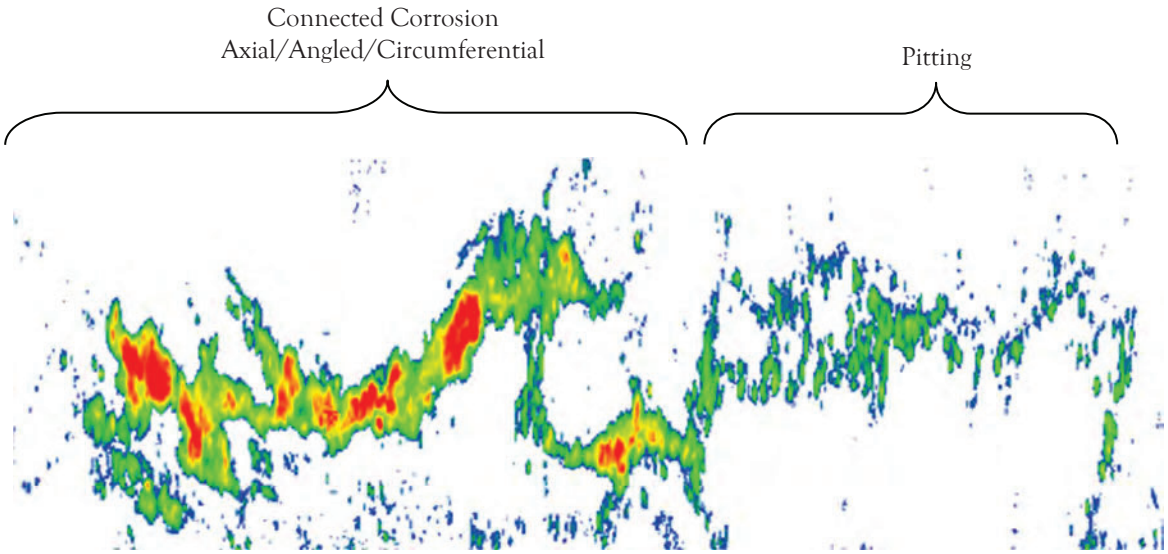

Figure 19: Connected complex corrosion laser scan

Figure 20 illustrates one of the categories identified, that of a deeper, axially oriented, area of metal loss within a larger area of general or circumferential corrosion. The challenges associated with this category lie as much with accurately resolving the circumferential aspects of the signal as with the axial principles outlined above.

The complex morphologies seen in real corrosion can prove challenging for both axial and transverse inspection technologies, but the triaxial sensors and associated principles enable much improved assessment of these complex areas.

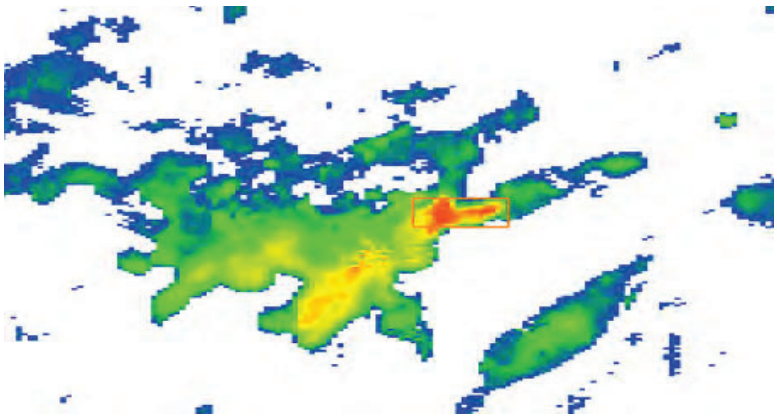

Figure 20: Axial corrosion within general corrosion

https://doi.org/10.52202/072781-0059

Depth prediction results

Given the selection criteria of the case study data set as "outliers" (outside of the 95% sizing performance Baker Hughes typically achieves for axial slotting) when using the standard analysis process, the initial depth performance had room for improvement with 47% of areas within +/-10%wt of actual depths (however noting that a +/-10%wt tolerance may not have been the specified tolerance for some of these features based on their actual defect dimensions).

After applying the improved categorisation and analysis techniques, the depth performance could be improved significantly to 83% within +/-10%. Figure 21 shows a unity plot of both the original and new predictions.

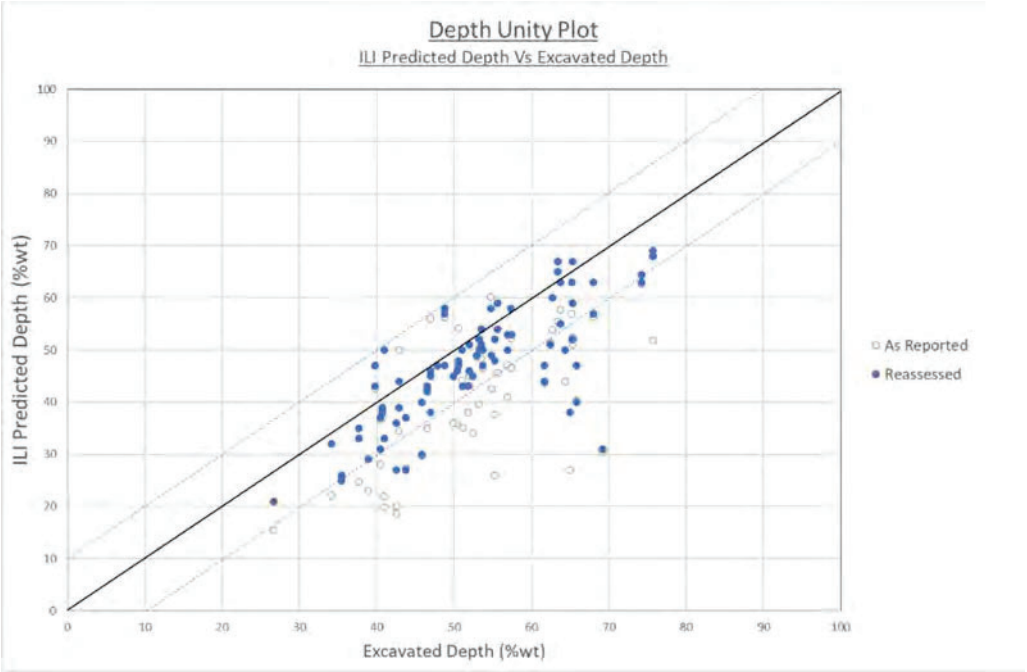

Figure 21: Depth performance unity plot

Note that Figure 21 shows the depth performance for all sites in the study; some sites had multiple deeper sections for which the depth could be assessed independently.

Pressure assessment and background corrosion

The pressure-based assessment of the sites was carried out using the tools available in proprietary DigCom software which allows depth profiles and burst pressures to be compared between NDE laser scan and ILI data. Figure 22 shows a typical visualisation of that data; the burst pressures were compared using RSTRENG (Effective Area Method) and LAPA techniques respectively on the laser scan and ILI data.

The initial predicted burst pressures were typically higher than the corresponding NDE values, and so most were non-conservative. The root causes for the underestimation were analysed and categorised for all sites, and it was common for multiple causal factors to be present.

https://doi.org/10.52202/072781-0059

Peak depth under calling is certainly associated with non-conservative burst pressures but for larger areas it is often not the critical factor. In Figure 22 for example, the peak depth and overall depth profile are accurately predicted in the ILI data (on the lower profile), and the variation in burst pressure is driven by the absence of low level or "background" corrosion between the corrosion boxes detected by the ILI decreasing the effective length. The treatment of the "connecting" low level corrosion was often critical to accurate burst pressure prediction.

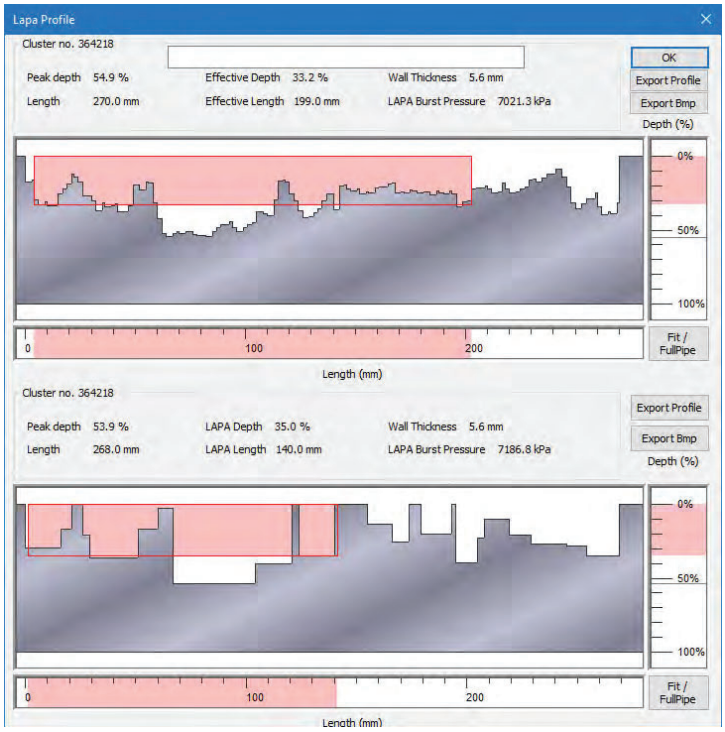

Figure 22: Depth profile and burst pressure comparison software visualisatio

n

Similar to the depth assessment, techniques were identified to recognise and address each of the root causes for under calling predicated pressures. In particular, updated techniques to measure or assess the extent, depth and impact of "background" corrosion were developed. In basic terms, the extent of this background is often associated with the "outside" poles of the ILI signal and may affect the depth sizing of any corrosion features contained within it. Figure 23 shows a subsection of the data shown in Figure 18, with the background corrosion poles identified, the arrow indicates the full extent of the corrosion.

https://doi.org/10.52202/072781-0059

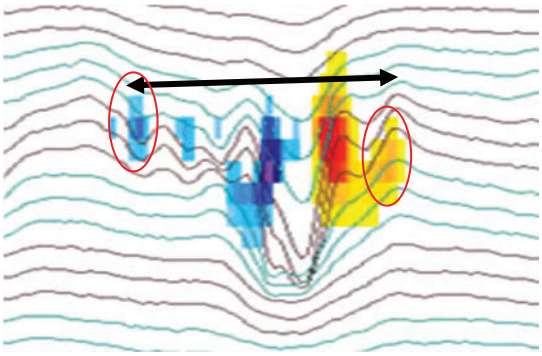

Figure 23: Background corrosion signal identifiers

Following assessment of the background corrosion on selected sites, the performance against an NDE corrosion depth estimated from the laser scan profiles was performed, and it was found that the accuracy was within 5%wt for all but one feature (Figure 24). The high accuracy is partially explained in that depth of these areas is usually relatively low level compared to associated pitting, slots, or grooves. Despite the shallow depth, the length of the background corrosion can have a significant effect on the burst pressure, and so accuracy is important.

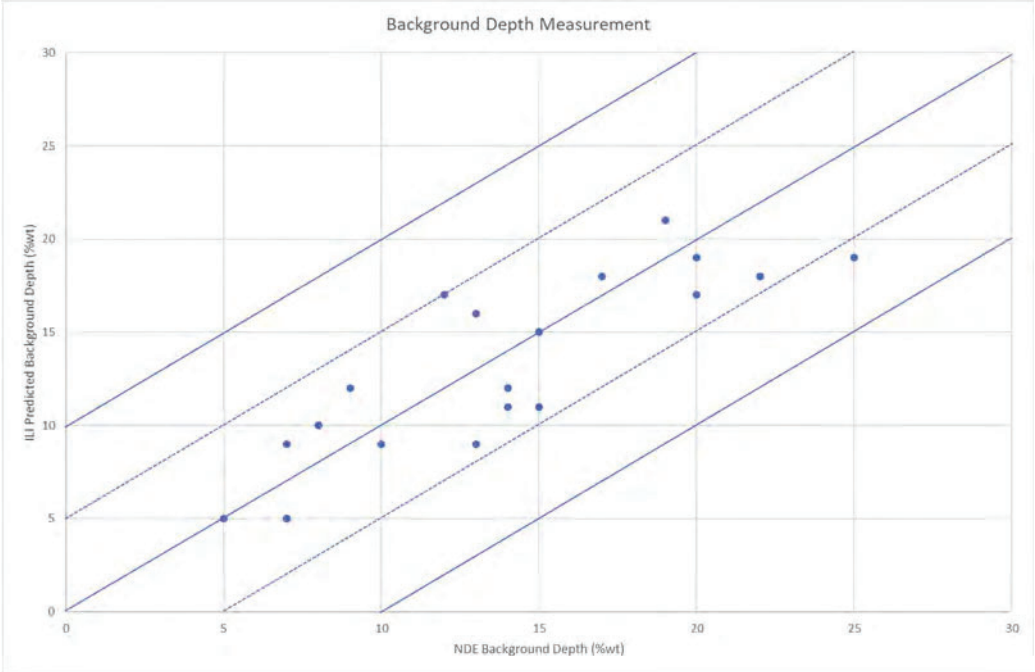

Figure 24: Background corrosion performance on selected sites

https://doi.org/10.52202/072781-0059

Pressure assessment results

The results of the pressure assessment are shown in the unity plot in Figure 25. In general, the original burst pressures were non-conservative due the factors described above, with only 37% of the sites being within 500 kPa of the laser scan derived value. After re-assessment with the revised process, 77% of the sites were within 500 kPa.

Note the number of points assessed is lower than the total number of sites in the study as the small area of some sites meant the burst pressure was purely depth driven, and the data below in Figure 25 is focused on the more complex larger corrosion areas where the pressure outliers were more pronounced.

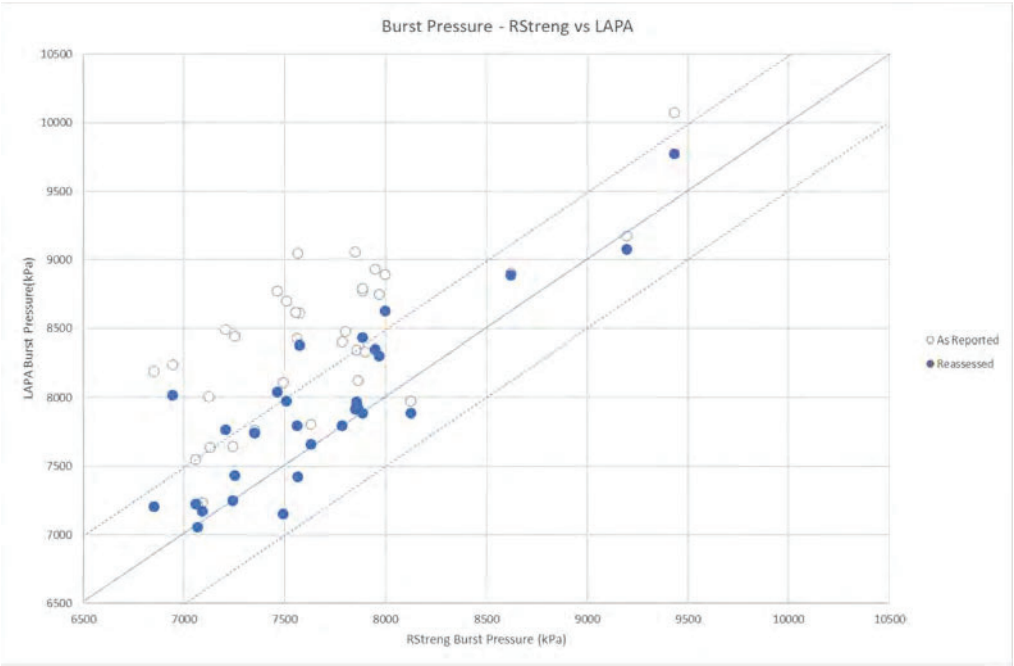

Figure 25: Burst pressure performance on selected sites

Conclusion

The case study described in this paper was based specifically on axial areas of corrosion that are outliers using the current Baker Hughes analysis process. The study demonstrated more accurate predictions in both peak depth and burst pressure are possible even on these complex areas by 1) using all the data available from the triaxial sensors; 2) using standard triaxial MFL data analysis principles used and adopted routinely with the technology but within a revised and targeted analysis process. Also, that the revised triaxial data analysis methods result in higher accuracy performance than either standard analysis using single axis axial or transverse MFL ILI systems.

The data set used was relatively small in around 50 sites but was diverse and representative of complex axial oriented corrosion and furthermore that the principals used are widely applicable. The data was not blinded or separated into test and training data; however, there was separation between

https://doi.org/10.52202/072781-0059

phases of deriving an updated process and applying the specified process to the sites to obtain the re-assessed predictions. The study is being followed up by blind tests to replicate and validate the results.

Baker Hughes maintains a database of hundreds of thousands of dig results including the ILI signal data and all field metadata. The database features can be labelled, categorised and are easily searchable; this data set is used to measure ILI performance, highlight opportunities for improvement, and support future development. The data from the initial study can be complemented with further axial sites from the database, and the categorisations from the study added to the database to enable larger scale validation and support continuous improvement efforts.

References

1. Specifications and requirements for in-line inspection of pipelines, Pipeline Operators Forum, November 2021.

2. In-line Inspection Systems Qualification, API Standard 1163, Third Edition, September 2021.

3. Sutherland, J., Bluck, M., Pearce, J. Quick, E. "Validation of latest generation MFL In-Line inspection technology leads to improved detection and sizing specification for pinholes, pitting, axial grooving and axial slotting", IPC2010-311224, 8th International Pipeline Conference 2010.

4. Feng, Q. Gu, B., Sutherland, J., Tao, C., Wei, Y., "Evolution of Triax Magnetic Flux Leakage Inspection for Mitigation Of Spiral Weld Anomalies" International Pipeline Conference, Paper No. 2010-31116, Calgary, September 2010.

5. Elliott, J., Farnie, S., Hurd, G., Sutherland, J., "Advancing In-line Inspection Technology and Pipeline Risk Management Through Advanced Analytics of Big Data", Clarion Technical Conferences and Tiratsoo Technical, Pipeline Pigging and Integrity Management Conference 2019.

https://doi.org/10.52202/072781-0059

https://doi.org/10.52202/072781-0059